



Photolysis and oxidation by OH radicals of two carbonyl nitrates: 4-nitrooxy-2-butanone and 5-nitrooxy-2-pentanone

Bénédicte Picquet-Varrault¹, Ricardo Suarez-Bertoa², Marius Duncianu³, Mathieu Cazaunau¹, Edouard Pangui¹, Marc David¹, and Jean-François Doussin¹

¹LISA, UMR CNRS 7583, Université Paris-Est Créteil, Université de Paris, Institut Pierre Simon Laplace (IPSL), Créteil, France

²European Commission Joint Research Centre (JRC), Ispra, Italy

³Interscience Belgium, Louvain-la-Neuve, Belgium

Correspondence: Bénédicte Picquet-Varrault (benedicte.picquet-varrault@lisa.u-pec.fr)

Received: 5 September 2019 – Discussion started: 20 September 2019

Revised: 19 November 2019 – Accepted: 27 November 2019 – Published: 14 January 2020

Abstract. Multifunctional organic nitrates, including carbonyl nitrates, are important species formed in NO_x-rich atmospheres by the degradation of volatile organic compounds (VOCs). These compounds have been shown to play a key role in the transport of reactive nitrogen and, consequently, in the ozone budget; they are also known to be important components of the total organic aerosol. However, very little is known about their reactivity in both the gas and condensed phases. Following a previous study that we published on the gas-phase reactivity of α -nitrooxy ketones, the photolysis and reaction with OH radicals of 4-nitrooxy-2-butanone and 5-nitrooxy-2-pentanone (which are a β -nitrooxy ketone and γ -nitrooxy ketone, respectively) were investigated for the first time in simulation chambers. The photolysis frequencies were directly measured in the CESAM chamber, which is equipped with a very realistic irradiation system. The $j_{\text{nitrate}}/j_{\text{NO}_2}$ ratios were found to be $(5.9 \pm 0.9) \times 10^{-3}$ for 4-nitrooxy-2-butanone and $(3.2 \pm 0.9) \times 10^{-3}$ for 5-nitrooxy-2-pentanone under our experimental conditions. From these results, it was estimated that ambient photolysis frequencies calculated for typical tropospheric irradiation conditions corresponding to the 1 July at noon at 40° N (overhead ozone column of 300 and albedo of 0.1) are $(6.1 \pm 0.9) \times 10^{-5} \text{ s}^{-1}$ and $(3.3 \pm 0.9) \times 10^{-5} \text{ s}^{-1}$ for 4-nitrooxy-2-butanone and 5-nitrooxy-2-pentanone, respectively. These results demonstrate that photolysis is a very efficient sink for these compounds with atmospheric lifetimes of few hours. They also suggest that, similarly to α -nitrooxy ketones, β -nitrooxy ketones have enhanced UV absorption cross sections and quan-

tum yields equal to or close to unity and that γ -nitrooxy ketones have a lower enhancement of cross sections, which can easily be explained by the larger distance between the two chromophore groups. Thanks to a product study, the branching ratio between the two possible photodissociation pathways is also proposed. Rate constants for the reaction with OH radicals were found to be $(2.9 \pm 1.0) \times 10^{-12}$ and $(3.3 \pm 0.9) \times 10^{-12} \text{ cm}^3 \text{ molecule}^{-1} \text{ s}^{-1}$, respectively. These experimental data are in good agreement with rate constants estimated by the structure–activity relationship (SAR) of Kwok and Atkinson (1995) when using the parametrization proposed by Suarez-Bertoa et al. (2012) for carbonyl nitrates. Comparison with photolysis rates suggests that the OH-initiated oxidation of carbonyl nitrates is a less efficient sink than photodissociation but is not negligible in polluted areas.

1 Introduction

Organic nitrates play an important role as sinks or temporary reservoirs of NO_x, as well as in ozone production in the atmosphere (Perring et al., 2013, 2010; Ito et al., 2007). They are formed by the degradation of volatile organic compounds (VOCs) in the presence of NO_x via two main processes:

- i. the reaction of the peroxy radical, produced by the oxidation of VOCs, with NO. The major pathway is generally Reaction (R1a), which leads to NO₂ formation. Reaction (R1b) is a minor channel, but it becomes gradu-

ally more important with increasing peroxy radical carbon chain length (Atkinson and Arey, 2003; Finlayson-Pitts and Pitts Jr., 2000).



- ii. The reaction of unsaturated VOCs with the NO_3 radical, which proceeds mainly by the addition of the nitrate radical on the double bond to produce nitro-alkyl radicals that can evolve into organic nitrates.

Among the organic nitrates, a variety of multifunctional species such as hydroxy-nitrates, carbonyl-nitrates, and dinitrates are formed. The formed species have been shown to significantly contribute to the nitrogen budget in both rural and urban areas (Perring et al., 2013). Beaver et al. (2012) observed that carbonyl nitrates, formed as second-generation nitrates from isoprene, are an important fraction of the total organic nitrates observed over Sierra Nevada in summer. These observations are supported by several studies that investigated the photooxidation of isoprene in simulation chambers (Paulot et al., 2009; Müller et al., 2014). These multifunctional organic nitrates are also semi-volatile/nonvolatile and highly soluble species; thus, they are capable of partitioning into the atmospheric condensed phases (droplets and aerosols). Numerous field observations of the chemical composition of atmospheric particles have shown that organic nitrates represent a significant fraction (up to 75 % in mass) of the total organic aerosol (OA), demonstrating that these species are important components of total OA (Ng et al., 2017).

Several modeling studies have also confirmed that multifunctional organic nitrates, in particular isoprene nitrates, play a key role in the transport of reactive nitrogen and, consequently, in the formation of ozone and other secondary pollutants at regional and global scales (Horowitz et al., 2007; Mao et al., 2013; Squire et al., 2015). In particular, Mao et al. (2013) performed simulations based on data from the ICARTT (International Consortium for Atmospheric Research on Transport and Transformation) aircraft campaign across the eastern US in 2004. They showed that organic nitrates, which are mainly composed of secondary organic nitrates, including a large fraction of carbonyl nitrates, provide an important pathway for exporting NO_x from the US's boundary layer, even exceeding the export of peroxyacyl nitrates (PANs). However, these modeling studies also point out the need for additional experimental data to better describe the sinks in both gas and condensed phases of multifunctional organic nitrates in models.

Recent experimental studies have revealed that hydrolysis in the aerosol phase may be a very efficient sink of organic nitrates in the atmosphere (Bean and Hildebrand Ruiz, 2016; Rindelaub et al., 2015). These studies also suggest that the rate of these reactions strongly depends on the organic nitrate chemical structure and that additional work is needed to

better understand these processes. In the gas phase, photolysis and reaction with the OH radical are expected to dominate the fate of organic nitrates (Roberts, 1990; Turberg et al., 1990). In a previous study, we measured the photolysis frequencies and the rate constants for the OH oxidation of three carbonyl nitrates (α -nitrooxyacetone, 3-nitrooxy-2-butanone, and 3-methyl-3-nitrooxy-2-butanone), and we showed that photolysis is the dominant sink for these compounds (Suarez-Bertoa et al., 2012). By comparison with absorption cross sections provided by Barnes et al. (1993), Müller et al. (2014) suggested the following: (i) that the α -nitrooxy ketones have enhanced absorption cross sections, due to the interaction between the $\text{C}=\text{O}$ and the ONO_2 chromophore groups; and (ii) that the photolysis quantum yield is close to unity and $\text{O}-\text{NO}_2$ dissociation is the likely major channel. They also showed that this enhancement was larger at the higher wavelengths, where the absorption by the nitrate chromophore is very small. Therefore, they concluded that the absorption by the carbonyl group was enhanced due to the neighboring nitrate group.

These results are significant as they demonstrate that photolysis frequencies of these multifunctional species cannot be calculated as the sum of the monofunctional species' (ketone + alkyl nitrate) frequencies. However, only α -nitrooxy ketones were studied, which means that the question of the persistence of the enhancement effect when the distance between the two functional groups increases remains. More recently, Xiong et al. (2016) studied the atmospheric degradation (photolysis, OH oxidation, and ozonolysis) of *trans*-2-methyl-4-nitrooxy-2-buten-1-al (also called 4,1-isoprene nitrooxy enal) in order to better assess – as a model compound – the reactivity of carbonyl nitrates formed by the NO_3 -initiated oxidation of isoprene. This compound has a conjugated chromophore $\text{C}=\text{C}-\text{C}=\text{O}$ in the β position of the nitrate group. The authors measured the absorption cross sections of the nitrooxy enal and compared them to those of the monofunctional species, i.e., methacrolein and isopropyl nitrate. They concluded that molecules containing β -nitrooxy ketone functionalities also have enhanced UV absorption cross sections. They also studied the kinetic and mechanisms for the oxidation of nitrooxy enal by OH and O_3 . They conclude that photolysis and reaction with OH are the two main loss processes of *trans*-2-methyl-4-nitrooxy-2-buten-1-al, leading to a tropospheric lifetime of less than 1 h.

Given the large contribution of carbonyl nitrates to the organic nitrate pool and the importance of their photochemistry for the NO_x budget, we present a study that aims at providing new experimental data on the gas-phase reactivity of these compounds. The study also seeks to disclose how photolysis and reaction with OH radical of carbonyl nitrates are affected by modifying their carbon chain length and the position of the two functional groups present in their molecular structure. Here, we provide the first photolysis frequencies and also the first rate constants for the OH oxidation of

two carbonyl nitrates: 4-nitrooxy-2-butanone and 5-nitrooxy-2-pentanone.

2 Experimental section

Reactants syntheses

As a common OH precursor in simulation chamber experiments, isopropyl nitrite was synthesized by dropwise addition of a dilute solution of H_2SO_4 into a mixture of NaNO_2 and isopropanol, following the classical protocol proposed by Taylor et al. (1980).

On the contrary, 4-nitrooxy-2-butanone and 5-nitrooxy-2-pentanone were synthesized for the first time. Great care was taken to develop a robust process: 4-nitrooxy-2-butanone and 5-nitrooxy-2-pentanone syntheses are based on Kames' method (Kames et al., 1993). This method consists of a liquid-/gas-phase reaction where the corresponding hydroxy-ketone reacts with NO_3 radicals released from the dissociation of N_2O_5 . The N_2O_5 was preliminarily synthesized in a vacuum line by reaction of NO_2 with ozone, as described by Scarfoglierio et al. (2006). The synthesis of the carbonyl nitrate is performed in a dedicated vacuum line connected to two bulbs: one containing the hydroxy-ketone, and the other containing N_2O_5 . The two bulbs are also connected to each other. In a first step, the bulbs are placed in a liquid N_2 cryogenic trap and pumped in order to remove air and impurities. In a second step, the cryogenic trap is removed from the bulb containing N_2O_5 in order to let it warm and transfer into the bulb containing the hydroxy-ketone. Then, the bulb containing both reactants is stirred and kept at 0°C for approximately 1 h. Finally, the resulting carbonyl nitrate and nitric acid, its coproduct, were separated by liquid–liquid extraction using dichloromethane and water. The carbonyl nitrate structure and purity were verified by FT-IR and GC-MS. Traces of impurities (HCOOH and CH_3COOH) were detected. The carbonyl nitrates were stored at -18°C and under nitrogen atmosphere to prevent them from decomposing. Infrared spectra of 4-nitrooxy-2-butanone and 5-nitrooxy-2-pentanone are available from the EUROCHAMP Data Centre (<https://data.eurochamp.org>, last access: 8 January 2020).

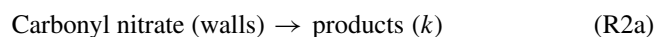
3 Determination of photolysis frequencies

The photolysis frequencies of the two carbonyl nitrates were determined by carrying out experiments in the CESAM simulation chamber, which is only briefly described here as detailed information can be found in Wang et al. (2011). The chamber consists of a 4.2 m^3 stainless-steel vessel equipped with a multiple-reflection optical system interfaced to a FTIR spectrometer (Bruker TENSOR 37) and also with NO , NO_2 , and O_3 analyzers (HORIBA) to monitor the composition of the gas phase. The chamber is also equipped with three high pressure xenon arc lamps (MH-Diffusion, MacBeam 4000)

which are combined with 7 mm Pyrex filters. This irradiation device provides a very realistic actinic flux (see comparison with the solar actinic flux in Fig. S1 in the Supplement) which allows for the measurement of photolysis frequencies under realistic conditions (Wang et al., 2011; Suarez-Bertoa et al., 2012). However, as the intensity of the irradiation in the CESAM chamber is lower than that in the ambient environment, $j_{\text{nitrate}}/j_{\text{NO}_2}$ ratios were provided in order to allow for the calculation of j_{nitrate} under various sunlight conditions. Hence, the intensity of the actinic flux was determined by measuring the photolysis frequency of NO_2 (J_{NO_2}) during dedicated experiments. A total of 400 ppbv of NO_2 in 1000 mbar of N_2 was injected into the CESAM chamber and kept in the dark for 20 min. The lights were then turned on for 20 min, and finally the mixture was left in the dark for an additional 20 min period. The photolysis frequency was subsequently determined using a kinetic numerical model developed for previous NO_x photooxidation experiments in the CESAM chamber (Wang et al., 2011). The fitting of modeled values from the measured data provided a NO_2 photolysis frequency equal to $2.2 \times 10^{-3}\text{ s}^{-1}$ (± 0.01 , 2σ error).

During a typical experiment, carbonyl nitrates were introduced into the chamber which was preliminarily filled at atmospheric pressure with N_2/O_2 (80/20). For the injection, the bulb containing the carbonyl nitrate was connected to the chamber and slightly heated while it was flushed with N_2 . Mixing ratios of carbonyl nitrates ranged from hundreds of parts per billion to parts per million. Because carbonyl nitrates may decompose during the injection, large amounts of NO_2 (hundreds of parts per billion) were present in the mixture. Cyclohexane was also added to the mixture as an OH scavenger with mixing ratios of approximately 4 ppm. Considering the fact that cyclohexane is approximately twice as reactive with OH radicals as carbonyl nitrates (see Sect. 4), it was estimated that between 80 % and 98 % of the OH radicals were scavenged (depending on the experiment considered). The mixture was kept under dark conditions for 2 h to enable assessment of the impact of the reactor's walls and to minimize their effects by passivation. Then, the mixture was irradiated for 3 h. For most experiments, the mixture was finally left in the dark for approximately 1 h after the irradiation period to allow for verification of whether wall losses were constant during the entire duration of the experiment.

During the experiment, the carbonyl nitrate loss processes can be described as



$$-\frac{d[\text{nitrate}]}{dt} = (j_{\text{nitrate}} + k) \times [\text{nitrate}] \quad (1)$$

$$\ln[\text{nitrate}]_t = \ln[\text{nitrate}]_0 - (k + j_{\text{nitrate}}) \times t. \quad (2)$$

Reaction (R2a) had to be added to the system to take the interaction or adsorption of the carbonyl nitrates on the

stainless-steel walls of the CESAM chamber during the experiments into account. By plotting $\ln[\text{nitrate}]_t$ vs. time, where $[\text{nitrate}]_t$ is the concentration of the carbonyl nitrate at time t , a straight line is obtained with a slope of $(k + j_{\text{nitrate}})$. The same approach was applied to each of the “dark” periods, before and after irradiation, to determine their respective dark decay rates, namely k_{before} and k_{after} , and k was calculated as the average of k_{before} and k_{after} for each experiment. Finally, j_{nitrate} was calculated as the difference between the loss rate during the irradiation period $(k + j_{\text{nitrate}})$ and the averaged loss rate during the dark periods (k) .

The uncertainties were calculated by adding the respective statistical errors (2σ) associated with the dark and light periods, with the former set as the average of the uncertainties determined for both dark periods (i.e., before and after irradiation). However, for some experiments, it was observed that the dark decay rate before irradiation was significantly higher than the one after, suggesting that the wall loss process is more complex than a “simple” first-order process and may decrease with time due to a passivation of the walls. More generally, interactions of gases with walls remain poorly understood and are currently subject to intensive investigations by the scientific community. Here, in order to determine wall loss decays which are as representative as possible of that during the irradiation period, the first experimental points (after the injection of the carbonyl nitrate) were not taken into account for the linear fit leading to the determination of k_{before} . In addition, the uncertainty was not calculated using the approach detailed above, with the statistical error being too low compared with the difference between k_{before} and k_{after} . Thus, the uncertainty was estimated in order to include the lowest and the highest J_{nitrate} values calculated with the highest and the lowest k values, respectively. Finally, the overall uncertainty associated with the photolysis frequency of each of the carbonyl nitrates was calculated as the average of the uncertainties obtained for each experiment, divided by the square root of the number of experiments (2 or 3).

3.1 Determination of the OH-oxidation rate constants

The kinetic experiments for the OH oxidation of the carbonyl nitrates were performed in the CSA chamber at room temperature and atmospheric pressure, in a mixture of N_2/O_2 (80/20). The chamber consists of a 977 L Pyrex™ vessel irradiated by two sets of 40 fluorescent tubes (Philips TL05 and TL03) that surround the chamber. The emissions of these black lamps are centered on 360 and 420 nm, respectively. The chamber is equipped with a multiple-reflection optical system with a path length of 180 m interfaced to a FTIR spectrometer (VERTEX 80 from Bruker). Additional details about this smog chamber are given elsewhere (Doussin et al., 1997; Duncianu et al., 2017).

The relative rate technique was used to determine the rate constant for the OH oxidation of the carbonyl nitrates with methanol as reference compound. We used

the IUPAC recommended value $k_{(\text{methanol}+\text{OH})} = (9.0 \pm 1.8) \times 10^{-13} \text{ cm}^3 \text{ molecule}^{-1} \text{ s}^{-1}$ (<http://iupac.pole-ether.fr/>, last access: 8 January 2020). Hydroxyl radicals were generated by photolyzing isopropyl nitrite. Initial mixing ratios of reactants (carbonyl nitrate, isopropyl nitrite, methanol, and NO) were in the parts per million range. As previously described, the carbonyl nitrate was introduced into the chamber by connecting the bulb to the chamber and by slightly heating and flushing it with N_2 . NO was added to the mixture in order to enhance the formation of OH radicals by reaction with HO_2 radicals which are formed by isopropyl nitrite photolysis. All experiments were conducted during a 1 h period of continuous irradiation.

Prior to the experiments, it was verified that photolysis and wall losses of the studied compounds were negligible under our experimental conditions. This can be explained by the facts that (i) the irradiation system of the CSA chamber emits photons at significantly higher wavelengths than the CESAM chamber, and (ii) the walls of the chamber are made of Pyrex which is more chemically inert than stainless steel. Therefore, it was assumed that reaction with OH is the only fate of both the studied compound (carbonyl nitrate) and the reference compound (methanol) and that neither of these compounds is reformed at any stage during the experiment. Based on these hypotheses, it can be shown that

$$\ln \frac{[\text{nitrate}]_0}{[\text{nitrate}]_t} = \frac{k_{\text{nitrate}}}{k_{\text{methanol}}} \times \frac{[\text{methanol}]_0}{[\text{methanol}]_t}, \quad (3)$$

where $[\text{nitrate}]_0$ and $[\text{methanol}]_0$, and $[\text{nitrate}]_t$ and $[\text{methanol}]_t$ stand for the concentration of the carbonyl nitrate and the reference compound at times 0 and t , respectively. The plot $\ln([\text{nitrate}]_0/[\text{nitrate}]_t)$ vs. $\ln([\text{methanol}]_0/[\text{methanol}]_t)$ is linear with a slope equal to $k_{\text{nitrate}}/k_{\text{methanol}}$ and an intercept of zero. The uncertainty on k_{nitrate} was calculated by adding the relative uncertainty corresponding to the statistical error on the linear regression (2σ) and the error on the reference rate constant (here 20 % for methanol).

3.2 Chemicals and gases

Dry synthetic air was generated using N_2 (from liquid nitrogen evaporation, > 99.995 % pure, < 5 ppm H_2O , Linde Gas) and O_2 (quality N45, > 99.995 % pure, < 5 ppm H_2O , Air Liquide). The chemicals obtained from commercial sources are as follows: NO (quality N20, > 99 % Air Liquide), NO_2 (quality N20, > 99 % Air Liquide), 4-hydroxy-2-butanone (95 % Aldich), 5-hydroxy-2-pentanone (95 % Aldich), cyclohexane (VWR), methanol (J.T. Baker), H_2SO_4 (95 % VWR), NaNO_2 (≥ 99 Prolabo), and isopropanol (VWR).

4 Results and discussion

4.1 Photolysis of carbonyl nitrates

Figure 1 presents the kinetic plots obtained for the two compounds, where $\ln[\text{nitrate}]$ was plotted as a function of time. A significant decrease was observed for both compounds during the dark period, before and after irradiation, suggesting that they adsorb or decompose on the walls. Thus, photolysis frequencies were calculated as the difference between the decay rates in the dark and that under irradiation (see Sect. 2.2). Results obtained for both compounds and for all experiments are given in Table 1. For 4-nitrooxy-2-butanone, photolysis frequencies are in good agreement despite the fact that decay rates in the dark differ from one experiment to another. For 5-nitrooxy-2-butanone, it can be seen that the decay rate in the dark before irradiation is significantly higher than the one after (in particular for experiments 3 and 4), suggesting that wall losses may decrease with time due to a passivation of the walls. Despite this, comparison of the three experiments showed good agreement. For CESAM irradiation conditions, the photolysis frequencies are $(1.3 \pm 0.2) \times 10^{-5} \text{ s}^{-1}$ for 4-nitrooxy-2-butanone and $(0.7 \pm 0.2) \times 10^{-5} \text{ s}^{-1}$ for 5-nitrooxy-2-pentanone. Hence, $j_{\text{nitrate}}/j_{\text{NO}_2}$ ratios were found to be $(5.9 \pm 0.9) \times 10^{-3}$ for 4-nitrooxy-2-butanone and $(3.2 \pm 0.9) \times 10^{-3}$ for 5-nitrooxy-2-pentanone.

In Table 2, these photolysis frequencies are compared to those we obtained in a previous study (Suarez-Bertoa et al., 2012) for 3-nitrooxy-2-propanone, 3-nitrooxy-2-butanone, and 3-methyl-3-nitrooxy-2-butanone using the same experimental conditions and methodology. Experimental photolysis frequencies have also been compared to those calculated using cross sections published in the literature and by assuming a quantum yield equal to unity. The intensity of the actinic flux in the CESAM chamber was determined by combining measurement of the spectrum of the lamps with a spectroradiometer and determination of j_{NO_2} by chemical actinometry (see Sect. 2.2). For 3-nitrooxy-2-propanone and 3-nitrooxy-2-butanone, cross sections were taken from Barnes et al. (1993). For 4-nitrooxy-2-butanone and 5-nitrooxy-2-pentanone, for which no data have been provided in the literature, cross sections were estimated using those for corresponding monofunctional species and by applying the enhancement factor (r_{nk}) obtained for 3-nitrooxy-2-propanone (Müller et al., 2014):

$$r_{nk} = \frac{s_{nk}}{s_n + s_k}, \quad (4)$$

where s_{nk} , s_n , and s_k are the absorption cross sections of the ketonitrate, the alkyl nitrate, and the ketone, respectively. For 4-nitrooxy-2-butanone, cross sections of 2-butanone and 1-butyl nitrate were taken from IUPAC (<http://iupac.pole-ether.fr/>, last access: 8 January 2020). For 5-nitrooxy-2-pentanone, cross sections of 2-pentanone ([\[mpic.de/spectral_atlas\]\(http://mpic.de/spectral_atlas\), last access: 15 November 2019\) and 1-pentyl nitrate \(Clemishaw et al., 1997\) were used. From these results, it can be observed that the experimental photolysis frequencies \(\$j_{\text{exp}}\$ \) obtained for 3-nitrooxy-2-propanone and 4-nitrooxy-2-butanone are very close and can be considered as equal within uncertainties. This suggests that the strong enhancement in the cross sections induced by the interaction between the two functional groups, which has been observed for \$\alpha\$ -nitrooxy ketones, also exists with the same amplitude for \$\beta\$ -nitrooxy ketones. This is confirmed by the fact the experimental value for 4-nitrooxy-2-butanone is in very good agreement with the calculated value, obtained by assuming that the enhancement factor is the same as that for 3-nitrooxy-2-propanone. Nonetheless, this effect seems to fade away when the two functions are one carbon further away. The experimental photolysis frequency obtained for 5-nitrooxy-2-pentanone is indeed significantly lower than those for 3-nitrooxy-2-propanone and 4-nitrooxy-2-butanone. It is also much lower than the \$J\$ value calculated by assuming the same enhancement factor as for 3-nitrooxy-2-propanone. This result suggests that the enhancement is significantly reduced for \$\gamma\$ -nitrooxy ketones even if it is probably not totally absent. This can easily be explained by the fact that the inductive effect of the nitrate group is expected to decrease when the distance between the functional groups increases. Another explanation would be that the quantum yield is significantly lower than unity. Finally, by comparing results for 3-nitrooxy-2-propanone, 3-nitrooxy-2-butanone, and 3-methyl-3-nitrooxy-2-butanone, it can be observed that photolysis frequencies increase with the substitution of the alkyl chain. From these kinetic data, it can be concluded that photolysis frequencies of \$\alpha\$ - and \$\beta\$ -nitrooxy ketones are much higher than those obtained when considering the sum of the photolysis frequencies for monofunctional species.](http://satellite.</p></div><div data-bbox=)

Products formed by the photolysis of the carbonyl nitrates were investigated using FTIR spectrometry. For both compounds, only peroxy acetyl nitrate (PAN) was detected. To calculate its formation yield, the concentration of PAN was plotted as a function of $-\Delta[\text{nitrate}]_{\text{photolysis}}$, i.e., the carbonyl nitrate loss rate due to photolysis. This loss rate was calculated by subtracting the loss rate measured during the dark period before the photolysis from that measured during the photolysis. Because the yield was calculated as the initial slope of the plot, the dark period before irradiation was considered to be more representative than the period after irradiation. The uncertainty on the yield was calculated by taking the uncertainties on the infrared absorption cross sections of PAN (10 %) and carbonyl nitrates (10 %) as well as the uncertainty on j into account (see Table 1). For 5-nitrooxy-2-pentanone, this uncertainty was quite large because the photolysis rate was relatively slow in comparison to the loss to the reactor walls. PAN formation yields obtained for both compounds are given in Table 1.

For 4-nitrooxy-2-butanone, PAN is formed with a yield equal to unity. Its formation can be explained by the dissoci-

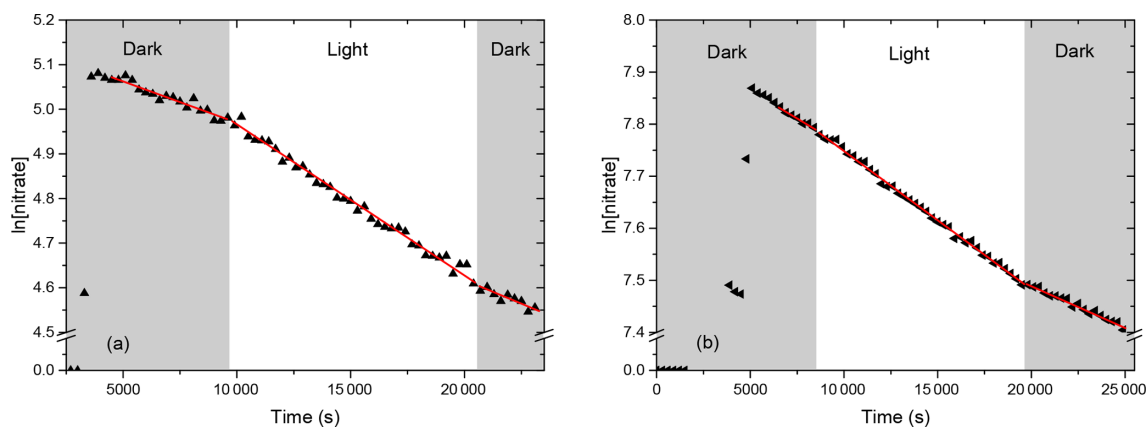


Figure 1. Kinetic plots for (a) the photolysis of 4-nitrooxy-2-butanone (experiment 2) and (b) the photolysis of 5-nitrooxy-2-pentanone (experiment 5). Red lines correspond to linear regressions.

Table 1. Photolysis frequencies and PAN yields for 4-nitrooxy-2-butanone and 5-nitrooxy-2-pentanone measured in the CESAM chamber.

Compound	Experiment	$k_{\text{before}}^{\text{a}}$ ($\times 10^{-5} \text{ s}^{-1}$)	$k_{\text{after}}^{\text{b}}$ ($\times 10^{-5} \text{ s}^{-1}$)	$(k + j_{\text{nitrate}})^{\text{c}}$ ($\times 10^{-5} \text{ s}^{-1}$)	$j_{\text{nitrate}}^{\text{d}}$ ($\times 10^{-5} \text{ s}^{-1}$)	PAN yield (%)
4-Nitrooxy-2-butanone	1	0.8 ± 0.1	–	2.1 ± 0.1	1.3 ± 0.2	100 ± 35
	2	1.9 ± 0.2	2.1 ± 0.1	3.3 ± 0.1	1.3 ± 0.3	100 ± 40
	Average				1.3 ± 0.2	100 ± 30
5-Nitrooxy-2-pentanone	3	2.0 ± 0.2	1.1 ± 0.2	2.3 ± 0.1	0.7 ± 0.4	13 ± 9
	4	1.9 ± 0.2	1.1 ± 0.1	2.2 ± 0.1	0.7 ± 0.4	13 ± 9
	5	2.1 ± 0.2	1.6 ± 0.2	2.7 ± 0.1	0.8 ± 0.3	23 ± 13
Average				0.7 ± 0.2	16 ± 8	

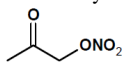
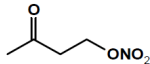
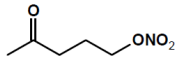
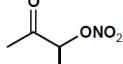
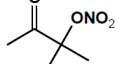
^{a,b} Dark decay rate due to wall loss, before and after irradiation; ^c decay rate during the irradiation period; ^d photolysis rate calculated as the difference between the decay rate during irradiation and the average dark decay rate.

ation of the C(O)–C bond, as shown in Scheme 1. This pathway also leads to the formation of the alkyl radical $\cdot\text{CH}_2\text{–CH}_2\text{ONO}_2$ which reacts with O_2 to form the corresponding peroxy radical, with the latter then evolving to the formation of the alkoxy by reaction with NO. Two pathways have been considered for the evolution of the alkoxy radical: (i) the decomposition that may lead to the formation of NO_2 and two molecules of HCHO and (ii) the reaction with O_2 that produces nitrooxy ethanal, also called ethanal nitrate ($\text{CH}_2(\text{ONO}_2)\text{–CH}(\text{O})$). Neither of these two products have been detected by FTIR. However, absorption bands of ethanal nitrate are expected to be very similar to those of the reactant; thus, it may be difficult to distinguish them. In addition, ethanal nitrate is expected to photodissociate much faster than the ketonitrate. The other photodissociation pathway is the cleavage of the O– NO_2 bond. It leads to the formation of the $\text{CH}_3\text{C}(\text{O})\text{CH}_2\text{CH}_2\text{O}\cdot$ radical which is expected to react with O_2 to form a dicarbonyl product. This product was not observed, which is in good agreement with the formation of PAN with a yield equal to unity by the other photodissociation pathway. It should be noticed that PAN has been

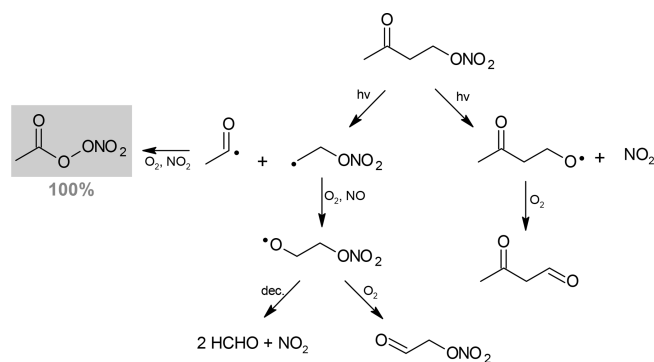
detected as a primary product, suggesting that its formation via the photolysis of the dicarbonyl product is not expected. In our experiments, it was not possible to measure the NO_2 formation yield because large amounts of NO_2 (hundreds of parts per billion) were introduced with the carbonyl nitrate (probably due to its decomposition during the injection).

As discussed above, as the enhancement in the cross sections is larger at the higher wavelengths, where absorption by the nitrate chromophore is very small, it was proposed by Müller et al. (2014) that the absorption by the carbonyl chromophore is enhanced due to the neighboring nitrate group. The authors also suggested that the photodissociation proceeds by a dissociation of the weak O– NO_2 bond, i.e., that a photon absorption by one chromophore (carbonyl group) causes dissociation in another part of the molecule (nitro group). This is not in line with what we observed in our study. From our experiments, we conclude that the photolysis of 4-nitrooxy-2-butanone proceeds mainly by a dissociation of the C(O)–C bond. In the former study on the photolysis of 3-nitrooxy-2-propanone, 3-nitrooxy-2-butanone, and 3-methyl-3-nitrooxy-2-butanone (Suarez-Bertoa et al., 2012),

Table 2. Comparison of the experimental photolysis frequencies of carbonyl nitrates with those calculated for CESAM irradiation conditions and by assuming a quantum yield equal to unity.

Compound	J_{exp} ($\times 10^{-5} \text{ s}^{-1}$)	J_{calc} ($\times 10^{-5} \text{ s}^{-1}$) ($\varphi = 1$)
3-Nitrooxy-2-propanone 	1.5 ± 0.1 (Suarez-Bertoa et al., 2012)	1.4 ^b
4-Nitrooxy-2-butanone 	1.3 ± 0.2 (This work)	1.6 ^a
5-Nitrooxy-2-pentanone 	0.7 ± 0.2 (This work)	1.8 ^a
3-Nitrooxy-2-butanone 	1.8 ± 0.1 (Suarez-Bertoa et al., 2012)	2.2 ^b
3-Methyl-3-nitrooxy-2-butanone 	2.31 ± 0.05 (Suarez-Bertoa et al., 2012)	ND

^a Calculated with estimated cross sections (see text); ^b calculated with experimental cross sections from the literature. ND: not determined

**Scheme 1.** Photolysis pathways of 4-nitrooxy-2-butanone. Detected products are indicated using a gray background, and their formation yield is given (in percent).

PAN and carbonyl compounds (formaldehyde, acetaldehyde and acetone, respectively) were detected as major products. However, the branching ratio of the two pathways (dissociation of O–NO₂ and C(O)–C bonds) could not be determined, as the formation of these products, in particular PAN, can be explained by the two pathways.

For 5-nitrooxy-2-pentanone, the formation yield of PAN has been observed to be much lower: 0.16 ± 0.08. As for 4-nitrooxy-2-butanone, its formation can be explained by the dissociation of the C(O)–C bond (see Scheme 2). This result

Table 3. Rate constants for the OH oxidation of 4-nitrooxy-2-butanone and 5-nitrooxy-2-pentanone.

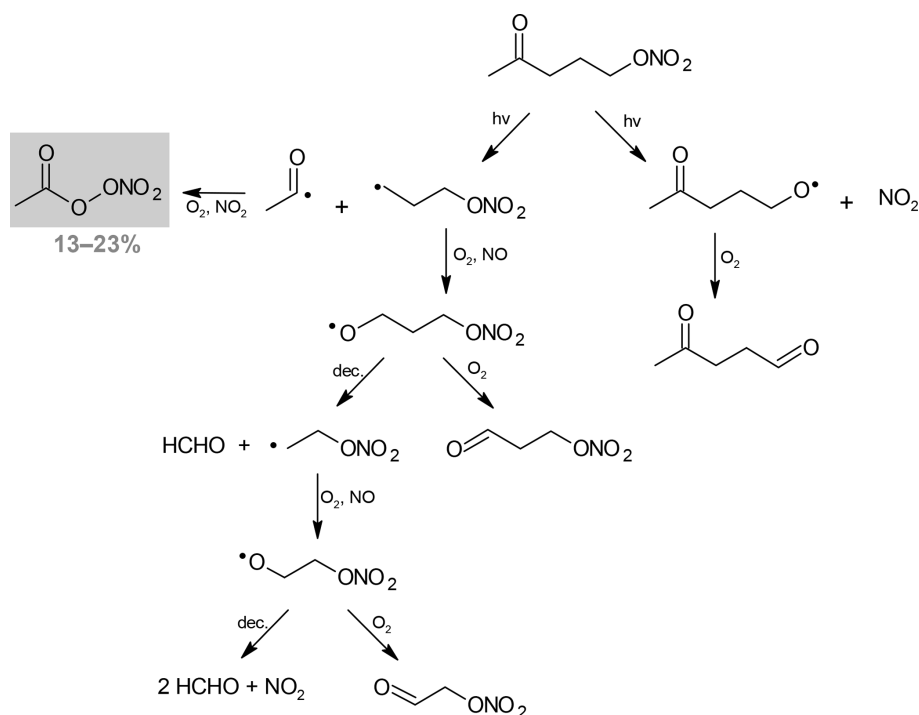
Compound	$k_{\text{nitrate}}/k_{\text{methanol}}$	$k_{\text{nitrate}} \times 10^{-12}$ ($\text{cm}^3 \text{ molecule}^{-1} \text{ s}^{-1}$)
4-Nitrooxy-2-butanone	3.25 ± 0.47	2.9 ± 1.0
5-Nitrooxy-2-pentanone	3.70 ± 0.28	3.3 ± 0.9

suggests that both dissociation pathways may occur and that O–NO₂ dissociation could be the major pathway. However, this was not confirmed by the detection of the dicarbonyl compound (2-oxo-pentanal) which is expected to be formed by this pathway. Despite the fact that no standard was available for this compound, no characteristic band was observed in the residual spectrum (after the subtraction of reactants and PAN spectra). Because the photolysis rate of 5-nitrooxy-2-pentanone is very low, we suspect that the concentration of this product is below the detection limit. Nevertheless, the low PAN yield is a strong indication that O–NO₂ dissociation may be the major pathway, contrary to what has been observed for 4-nitrooxy-2-butanone. This should be considered in the light of the low enhancement of absorption cross sections which has been assumed for this compound. Hence, in the case of γ -nitrooxy ketones, the enhancement of the absorption by the carbonyl chromophore seems to significantly decrease, leading to a lower branching ratio of the C(O)–C bond dissociation.

4.2 OH oxidation of carbonyl nitrates

Rate constants of the OH oxidation were measured for 4-nitrooxy-2-butanone and 5-nitrooxy-2-pentanone. Prior to the experiments, it was checked that the carbonyl nitrates did not photolyze nor decompose/adsorb on the walls of the chamber. Figure 2 represents the kinetic plots obtained for the two carbonyl nitrates. For each compound, several independent kinetic experiments were performed and data were combined to provide the $k_{\text{ketonitrate}}/k_{\text{methanol}}$ for each compound (see Fig. 2). In order to limit errors in the quantification of reactants due to the possible formation of carbonyl nitrates as products, only the very beginning of the experiments was taken into account for the kinetic plots. This explains the small number of experimental points. The obtained rate constants are given in Table 3. These data are, to our knowledge, the first determinations of the rate constants for the reaction of OH with these two carbonyl nitrates. From these data, it can be concluded that 4-nitrooxy-2-butanone and 5-nitrooxy-5-pentanone have similar reactivity towards OH radicals with rate constants equal to $(2.9 \pm 1.0) \times 10^{-12}$ and $(3.3 \pm 0.9) \times 10^{-12} \text{ cm}^3 \text{ molecule}^{-1} \text{ s}^{-1}$, respectively.

Rate constants provided in this study, as well as those previously reported for a series of α -nitrooxy-ketones (Suarez-Bertoa et al., 2012) have been compared to those estimated using structure–activity relationships (SARs) in Ta-



Scheme 2. Photolysis pathways of 5-nitrooxy-2-pentanone. Detected products are indicated using a gray background, and their formation yield is given (in percent).

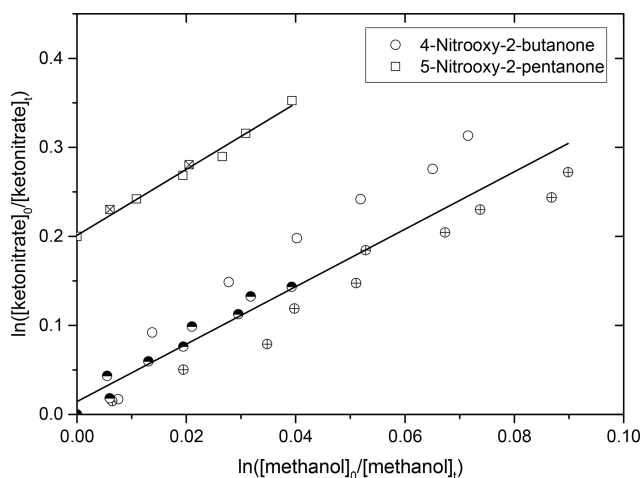


Figure 2. Kinetic plots for the oxidation of 4-nitrooxy-2-butanone and 5-nitrooxy-2-pentanone by OH radicals. For 5-nitrooxy-2-pentanone, data have been shifted by 0.2 on the y axis. Different symbols correspond to different experiments.

ble 4. Different SARs have been evaluated: (i) that developed by Kwok and Atkinson (1995) with updated factors $F(-\text{ONO}_2) = 0.14$ and $F(-\text{C}-\text{ONO}_2) = 0.28$ from Bedjanian et al. (2018); (ii) that developed by Kwok and Atkinson (1995) with updated factors $F(-\text{ONO}_2) = 0.8$ and $F(-\text{C}-\text{ONO}_2) = 0.1$ from Suarez-Bertoa et al. (2012); (iii) that developed by Neeb (2000) which proposes a different type

of parametrization and has been observed to be particularly accurate for oxygenated species; and (iv) that developed by Jenkin et al. (2018) which proposes a parametrization very similar to the one from Kwok and Atkinson (1995) and Bedjanian et al. (2018). The rate constant for 5-nitrooxy-2-pentanone is reasonably well reproduced by all SARs (within a factor of 2). For 4-nitrooxy-2-butanone, only the parametrization provided by Suarez-Bertoa et al. (2012) succeeds in reproducing the experimental value. This can be explained by the fact that this parametrization has been optimized for carbonyl nitrates, whereas the others have been developed using the entire dataset for compounds containing a nitrate group ($-\text{ONO}_2$) (Jenkin et al., 2018) or using the dataset for alkyl nitrates (Bedjanian et al., 2018). The main difference between these parameterizations is that in Suarez-Bertoa et al. (2012), the factor $F(-\text{ONO}_2)$ is much less deactivating than for the others. This could result from electronic interactions between the two functional groups. However, Suarez-Bertoa et al. (2012) noticed that their parametrization gives poor results for alkyl nitrates, suggesting that a specific parametrization has to be used for multifunctional species. This also suggests that the principle of SARs based on the group additivity method may not be suitable for multifunctional molecules.

From these experiments, several oxidation products have been detected: HCHO, PAN, and methylglyoxal for 4-nitrooxy-2-butanone, and HCHO, PAN, and 3-nitrooxypropanal for 5-nitrooxy-2-pentanone. However, their quan-

Table 4. Comparison of the experimental rate constants for the OH oxidation of carbonyl nitrates with those estimated by SARs.

Compound	k_{exp}	k_{SAR}	k_{SAR}	k_{SAR}	k_{SAR}
	$\times 10^{-13}$	Atkinson/Bedjanian ^a	Atkinson/Suarez ^b	Neeb ^c	Jenkin ^d
		$\times 10^{-13}$	$\times 10^{-13}$	$\times 10^{-13}$	$\times 10^{-13}$
3-Nitrooxy-2-propanone	6.7 ^e	2.0	6.6	5.8	2.5
3-Nitrooxy-2-butanone	10.1 ^e	4.5	13.2	6.8	3.7
3-Methyl-3-nitrooxy-2-butanone	2.6 ^e	4.0	2.1	2.4	4.3
4-Nitrooxy-2-butanone	29 ^f	8.1	30.9	8.7	8.1
5-Nitrooxy-2-pentanone	33 ^f	21.4	22.5	47.6	19.5

Rate constants are expressed in cubed centimeters per molecule per second ($\text{cm}^3 \text{ molecule}^{-1} \text{ s}^{-1}$); ^a SAR developed by Kwok and Atkinson (1995) with $F(-\text{ONO}_2)$ and $F(-\text{C}-\text{ONO}_2)$ from Bedjanian et al. (2018); ^b SAR developed by Kwok and Atkinson (1995) with $F(-\text{ONO}_2)$ and $F(-\text{C}-\text{ONO}_2)$ from Suarez-Bertoa et al. (2012); ^c SAR developed by Neeb (2000); ^d SAR developed by Jenkin et al. (2018); ^e experimental data from Suarez-Bertoa et al. (2012); ^f this work.

Table 5. Atmospheric lifetimes of carbonyl nitrates towards photolysis and reaction with OH radicals.

Compound	$J \times 10^{-5}$ ^a	τ_{hv}	$k_{\text{OH}} \times 10^{-12}$	τ_{OH}^b
	(s^{-1})	(h)	($\text{cm}^3 \text{ molecule}^{-1} \text{ s}^{-1}$)	(h)
4-Nitrooxy-2-butanone	6.1 ± 0.9	4	2.9 ± 1.0	48
5-Nitrooxy-2-pentanone	3.3 ± 0.9	8	3.3 ± 0.9	42

^a Photolysis frequencies estimated for a typical solar actinic flux (40°N , 1 July, noon) by applying a factor of 4.7 to those measured in the CESAM chamber (see Sect. 2.2); ^b estimated for $[\text{OH}] = 2 \times 10^6 \text{ molecule cm}^{-3}$.

tification was highly uncertain because the infrared spectra were complex due to the presence of methanol, isopropyl nitrite, impurities (in particular acetic acid), and their oxidation products. Dedicated mechanistic experiments should currently/in the near future be performed using HONO as the OH source in order to simplify the chemical mixture.

4.3 Atmospheric implications

Atmospheric lifetimes of the investigated compounds are presented in Table 5. The photolysis frequencies were estimated using $j_{\text{nitrate}}/j_{\text{NO}_2}$ ratios measured in this study and j_{NO_2} for typical tropospheric irradiation conditions corresponding to the 1 July at noon at 40°N (overhead ozone column of 300; albedo of 0.1; aerosol optical depth of 0.235; cloud optical depth of 0; TUV NCAR model, http://cpm.acom.ucar.edu/Models/TUV/Interactive_TUV/, last access: 15 November 2019). For $j_{\text{NO}_2} = 1.03 \times 10^{-2} \text{ s}^{-1}$, photolysis frequencies of carbonyl nitrates are as follows: $(6.1 \pm 0.9) \times 10^{-5} \text{ s}^{-1}$ for 4-nitrooxy-2-butanone and $(3.3 \pm 0.9) \times 10^{-5} \text{ s}^{-1}$ for 5-nitrooxy-2-pentanone. Under these irradiation conditions, lifetimes ($\tau_{hv} = 1/j$) were found to be 4 and 8 h, respectively. For OH oxidation, lifetimes ($\tau_{\text{OH}} = (1/(k_{\text{OH}}[\text{OH}])))$ were calculated using typical OH concentrations of $2 \times 10^6 \text{ molecule cm}^{-3}$ (Atkinson and Arey, 2003). They are both equal to approximately 2 d. Hence, it appears that photolysis is a more efficient sink than oxidation by OH radicals for 4-nitrooxy-2-butanone and 5-nitrooxy-2-pentanone. An identical conclusion was obtained for α -

nitrooxy carbonyls (Suarez-Bertoa et al., 2012; Barnes et al., 1993; Zhu et al., 1991). However, OH-initiated oxidation is not negligible, especially under polluted conditions where OH concentrations can be higher than $1 \times 10^7 \text{ molecule cm}^{-3}$.

In order to evaluate the impact of these carbonyl nitrates on the nitrogen budget and the transport of NO_x , it is crucial to determine whether their atmospheric sinks, here mainly photolysis, release NO_2 or not. For 4-nitrooxy-2-butanone, we observed that the photolysis proceeds mainly by a dissociation of the $\text{C}(\text{O})-\text{C}$ bond which does not necessarily lead to the release of NO_2 (see Scheme 2). In our experimental conditions (i.e., with high NO_2 mixing ratios), this pathway leads to the formation of PAN, which was detected with a yield equal to unity. Under a more realistic NO/NO_2 ratio, this reaction may also produce HCHO and CO_2 . The co-products of PAN, which could not be detected in our study, are expected to be formaldehyde + NO_2 or ethanal nitrate. Hence, one NO_2 molecule is released in the first hypothesis. Ethanal nitrate may react and undergo photolysis even faster than nitrooxy ketones and may thus lead to NO_2 release quite rapidly. However, as data on the reactivity of ethanal nitrate are not available in the literature, one cannot provide a definite conclusion. In the case of 5-nitrooxy-2-pentanone, the dissociation of the $\text{C}(\text{O})-\text{C}$ bond has been observed to be a minor pathway, suggesting that the major one, which was not directly observed here, is $\text{O}-\text{NO}_2$ dissociation. This process certainly leads to the release of NO_2 .

5 Conclusions

This paper presents the first study on the atmospheric reactivity of 4-nitrooxy-2-butanone and 5-nitrooxy-2-pentanone. Thanks to experiments in simulation chambers, photolysis frequencies and rate constants of the OH oxidation were measured for the first time. From these results, it is concluded that, similarly to α -nitrooxy ketones, β -nitrooxy ketones have enhanced UV absorption cross sections and quantum yields equal to or close to unity, making photolysis a very efficient sink for these compounds. Results obtained for 5-nitrooxy-2-pentanone, which is a γ -nitrooxy ketone, suggest a lower enhancement of cross sections, leading to slightly longer atmospheric lifetimes. This can easily be explained by the increasing distance between the two chromophore groups. Some photolysis products were also detected allowing estimating the branching ratio between the two possible pathways, i.e., the dissociation of the C(O)–C bond and that of the O–NO₂ bond. For 4-nitrooxy-2-butanone, we conclude that photolysis proceeds mainly by a dissociation of the C(O)–C bond, which does not necessarily lead to the release of NO₂. In the case of 5-nitrooxy-2-pentanone, our results suggest that the dissociation of the O–NO₂ bond is the major pathway. Reactivity of 4-nitrooxy-2-butanone and 5-nitrooxy-2-pentanone with OH radicals was also investigated. Both compounds have similar reactivity towards OH radicals, leading to lifetimes of approximately 2 d. Experimental rate constants are in good agreement with those estimated by the SAR proposed by Kwok and Atkinson (1995) when using the parametrization proposed by Suarez-Bertoa et al. (2012) for carbonyl nitrates. However, this specific parametrization does not allow for the reproduction of experimental data for monofunctional alkyl nitrates, suggesting that specific parametrization should be used for multifunctional species. Finally, these compounds are expected to be removed from the atmosphere fairly rapidly and to act as (only) temporary reservoirs of NO_x. If formed during the night, they could however contribute to longer-range transport of NO_x.

Data availability. Rate constants for the OH oxidation and photolysis frequencies of carbonyl nitrates are provided in Tables 1 and 3. They are also available through the Library of Advanced Data Products (LADP) of the EUROCHAMP data center (<https://data.eurochamp.org/data-access/gas-phase-rate-constants/>, last access: 10 January 2020, Picquet-Varrault et al., 2020a; <https://data.eurochamp.org/data-access/photolysis-frequencies-quantum-yields/>, last access: 10 January 2020, Picquet-Varrault et al., 2020b).

Simulation chamber experiments which were used to retrieve these parameters are available through the Database of Atmospheric Simulation Chamber Studies (DASCS) of the EUROCHAMP data center (<https://data.eurochamp.org/data-access/chamber-experiments/>, last access: 10 January 2020, Picquet-Varrault et al., 2020c).

Supplement. The supplement related to this article is available online at: <https://doi.org/10.5194/acp-20-487-2020-supplement>.

Author contributions. BPV coordinated the research project. BPV, RSB, and JFD designed the experiments in the simulation chambers. RSB performed the experiments with the technical support of MC and EP. RSB and MDa performed the organic syntheses. BPV, RSB, and MDu performed the data treatment and interpretation. BPV and RSB wrote the paper, and BPV was responsible for the final version of the paper. All coauthors revised the content of the original manuscript and approved the final version of the paper.

Competing interests. The authors declare that they have no conflict of interest.

Special issue statement. This article is part of the special issue “Simulation chambers as tools in atmospheric research (AMT/ACP/GMD inter-journal SI)”. It is not associated with a conference.

Acknowledgements. The authors thank Mila Ródenas (mila@ceam.es) (CEAM, Paterna-Valencia, Spain) for the development and free distribution of the ANIR software via the EUROCHAMP-2020 Data Centre website (<https://data.eurochamp.org>, last access: 8 January 2020).

Financial support. This work was supported by the French National Agency for Research (project no. ONCEM-ANR-12-BS06-0017-01) and by the European Commission’s Seventh Framework Programme (EUROCHAMP-2; grant no. 228335), H2020 Research Infrastructures (EUROCHAMP-2020; grant no. 730997).

Review statement. This paper was edited by Andreas Hofzumahaus and reviewed by two anonymous referees.

References

- Atkinson, R. and Arey, J.: Gas-phase tropospheric chemistry of biogenic volatile organic compounds: a review, *Atmos. Environ.*, 37, 197–219, 2003.
- Barnes, I., Becker, K. H., and Zhu, T.: Near UV absorption spectra and photolysis products of difunctional organic nitrates: possible importance as NO_x Reservoirs, *J. Atmos. Chem.*, 17, 353–373, 1993.
- Bean, J. K. and Hildebrandt Ruiz, L.: Gas–particle partitioning and hydrolysis of organic nitrates formed from the oxidation of α -pinene in environmental chamber experiments, *Atmos. Chem. Phys.*, 16, 2175–2184, <https://doi.org/10.5194/acp-16-2175-2016>, 2016.
- Beaver, M. R., Clair, J. M. St., Paulot, F., Spencer, K. M., Crouse, J. D., LaFranchi, B. W., Min, K. E., Pusede, S. E., Wooldridge, P.

- J., Schade, G. W., Park, C., Cohen, R. C., and Wennberg, P. O.: Importance of biogenic precursors to the budget of organic nitrates: observations of multifunctional organic nitrates by CIMS and TD-LIF during BEARPEX 2009, *Atmos. Chem. Phys.*, 12, 5773–5785, <https://doi.org/10.5194/acp-12-5773-2012>, 2012.
- Bedjanian, Y., Morin, J., and Romanias, M. N.: Reactions of OH radicals with 2-methyl-1-butyl, neopentyl and 1-hexyl nitrates. Structure-activity relationship for gas-phase reactions of OH with alkyl nitrates: An update, *Atmos. Environ.*, 180, 167–172, 2018.
- Clemmshaw, K. C., Williams, J., Rattigan, O. V., Shallcross, D. E., Law, K. S., and Cox, R. A.: Gas-phase ultraviolet absorption cross-sections and atmospheric lifetimes of several C₂–C₅ alkyl nitrates, *J. Photochem. Photobiol. A*, 102, 117–126, 1997.
- Doussin, J. F., Ritz, D., Durand-Jolibois, R., Monod, A., and Carlier, P.: Design of an environmental chamber for the study of atmospheric chemistry: New developments in the analytical device, *Analisis*, 25, 236–242, 1997.
- Duncanianu, M., David, M., Kartigeyane, S., Cirtog, M., Doussin, J.-F., and Picquet-Varrault, B.: Measurement of alkyl and multifunctional organic nitrates by proton-transfer-reaction mass spectrometry, *Atmos. Meas. Tech.*, 10, 1445–1463, <https://doi.org/10.5194/amt-10-1445-2017>, 2017.
- Finlayson-Pitts, B. J. and Pitts Jr., J. N.: *Chemistry of the Upper and Lower Atmosphere*, Academic Press, San Diego, 2000.
- Horowitz, L. W., Fiore, A. M., Milly, G. P., Cohen, R. C., Perring, A., Wooldridge, P. J., Hess, P. G., Emmons, L. K., and Lamarque, J.-F.: Observational constraints on the chemistry of isoprene nitrates over the eastern United States, *J. Geophys. Res.*, 112, D12S08, <https://doi.org/10.1029/2006JD007747>, 2007.
- Ito, A., Sillman, S., and Penner, J. E.: Effects of additional non-methane volatile organic compounds, organic nitrates, and direct emissions of oxygenated organic species on global tropospheric chemistry, *J. Geophys. Res.-Atmos.*, 112, D06309, <https://doi.org/10.1029/2005jd006556>, 2007.
- Jenkin, M. E., Valorso, R., Aumont, B., Rickard, A. R., and Wallington, T. J.: Estimation of rate coefficients and branching ratios for gas-phase reactions of OH with aliphatic organic compounds for use in automated mechanism construction, *Atmos. Chem. Phys.*, 18, 9297–9328, <https://doi.org/10.5194/acp-18-9297-2018>, 2018.
- Kames, J., Schurath, U., Flocke, F., and Volz-Thomas, A.: Preparation of organic nitrates from alcohols and N₂O₅ for species identification in atmospheric samples, *J. Atmos. Chem.*, 16, 349–359, 1993.
- Kwok, E. S. C. and Atkinson, R.: Estimation of Hydroxyl Radical Reaction Rate Constants for Gas-Phase Organic Compounds using a Structure-Reactivity Relationship: an update, *Atmos. Environ.*, 29, 1685–1695, 1995.
- Mao, J. Q., Paulot, F., Jacob, D. J., Cohen, R. C., Crouse, J. D., Wennberg, P. O., Keller, C. A., Hudman, R. C., Barkley, M. P., and Horowitz, L. W.: Ozone and organic nitrates over the eastern United States: Sensitivity to isoprene chemistry, *J. Geophys. Res.-Atmos.*, 118, 11256–11268, <https://doi.org/10.1002/jgrd.50817>, 2013.
- Müller, J.-F., Peeters, J., and Stavrou, T.: Fast photolysis of carbonyl nitrates from isoprene, *Atmos. Chem. Phys.*, 14, 2497–2508, <https://doi.org/10.5194/acp-14-2497-2014>, 2014.
- Neub, P.: Structure-Reactivity Based Estimation of the Rate Constants for Hydroxyl Radical Reactions with Hydrocarbons, *J. Atmos. Chem.*, 35, 295–315, 2000.
- Ng, N. L., Brown, S. S., Archibald, A. T., Atlas, E., Cohen, R. C., Crowley, J. N., Day, D. A., Donahue, N. M., Fry, J. L., Fuchs, H., Griffin, R. J., Guzman, M. I., Herrmann, H., Hodzic, A., Iinuma, Y., Jimenez, J. L., Kiendler-Scharr, A., Lee, B. H., Lueken, D. J., Mao, J., McLaren, R., Mutzel, A., Osthoff, H. D., Ouyang, B., Picquet-Varrault, B., Platt, U., Pye, H. O. T., Rudich, Y., Schwantes, R. H., Shiraiwa, M., Stutz, J., Thornton, J. A., Tilgner, A., Williams, B. J., and Zaveri, R. A.: Nitrate radicals and biogenic volatile organic compounds: oxidation, mechanisms, and organic aerosol, *Atmos. Chem. Phys.*, 17, 2103–2162, <https://doi.org/10.5194/acp-17-2103-2017>, 2017.
- Paulot, F., Crouse, J. D., Kjaergaard, H. G., Kroll, J. H., Seinfeld, J. H., and Wennberg, P. O.: Isoprene photooxidation: new insights into the production of acids and organic nitrates, *Atmos. Chem. Phys.*, 9, 1479–1501, <https://doi.org/10.5194/acp-9-1479-2009>, 2009.
- Perring, A. E., Bertram, T. H., Farmer, D. K., Wooldridge, P. J., Dibb, J., Blake, N. J., Blake, D. R., Singh, H. B., Fuelberg, H., Diskin, G., Sachse, G., and Cohen, R. C.: The production and persistence of \sum RONO₂ in the Mexico City plume, *Atmos. Chem. Phys.*, 10, 7215–7229, <https://doi.org/10.5194/acp-10-7215-2010>, 2010.
- Perring, A. E., Pusede, S. E., and Cohen, R. C.: An Observational Perspective on the Atmospheric Impacts of Alkyl and Multifunctional Nitrates on Ozone and Secondary Organic Aerosol, *Chem. Rev.*, 113, 5848–5870, <https://doi.org/10.1021/cr300520x>, 2013.
- Picquet-Varrault, B., Suarez-Bertoa, R., Duncanianu, M., Cazaunau, M., Pangui, E., David, M., and Doussin, J.-F.: Library of Advanced Data Products: Gas Phase Rate constants, available at: <https://data.eurochamp.org/data-access/gas-phase-rate-constants/>, last access: 10 January 2020a.
- Picquet-Varrault, B., Suarez-Bertoa, R., Duncanianu, M., Cazaunau, M., Pangui, E., David, M., and Doussin, J.-F.: Library of Advanced Data Products: Photolysis Frequencies & Quantum yields, available at: <https://data.eurochamp.org/data-access/photolysis-frequencies-quantum-yields/>, last access: 10 January 2020b.
- Picquet-Varrault, B., Suarez-Bertoa, R., Duncanianu, M., Cazaunau, M., Pangui, E., David, M., and Doussin, J.-F.: Database of Atmospheric Simulation Chamber Studies, available at: <https://data.eurochamp.org/data-access/chamber-experiments/>, last access: 10 January 2020c.
- Rindelaub, J. D., McAvey, K. M., and Shepson, P. B.: The photochemical production of organic nitrates from alpha-pinene and loss via acid-dependent particle phase hydrolysis, *Atmos. Environ.*, 100, 193–201, <https://doi.org/10.1016/j.atmosenv.2014.10.010>, 2015.
- Roberts, J. M.: The Atmospheric Chemistry of organic Nitrates, *Atmos. Environ. A-Gen.*, 24, 243–287, 1990.
- Scarfogliero, M., Picquet-Varrault, B., Salce, J., Durand-Jolibois, R., and Doussin, J.-F.: Kinetic and Mechanistic Study of the Gas-Phase Reactions of a Series of Vinyl Ethers with the Nitrate Radical, *J. Phys. Chem. A*, 110, 11074–11081, 2006.
- Squire, O. J., Archibald, A. T., Griffiths, P. T., Jenkin, M. E., Smith, D., and Pyle, J. A.: Influence of isoprene chemical mechanism on modelled changes in tropospheric ozone due to climate and land

- use over the 21st century, *Atmos. Chem. Phys.*, 15, 5123–5143, <https://doi.org/10.5194/acp-15-5123-2015>, 2015.
- Suarez-Bertoa, R., Picquet-Varrault, B., Tamas, W., Pangu, E., and Doussin, J. F.: Atmospheric Fate of a Series of Carbonyl Nitrates: Photolysis Frequencies and OH-Oxidation Rate Constants, *Environ. Sci. Technol.*, 46, 12502–12509, <https://doi.org/10.1021/es302613x>, 2012.
- Taylor, W. D., Allston, T. D., Moscato, M. J., Fazenkas, G. B., Koslowski, R., and Takacs, G. A.: Atmospheric Photodissociation lifetimes for nitromethane, methyl nitrite, and methyl nitrate, *Int. J. Chem. Kinet.*, 12, 231–240, 1980.
- Turberg, M. P., Giolando, D. M., Tilt, C., Soper, T., Mason, S., Davies, M., Klingensmith, P., and Takacs, G. A.: Atmospheric Photochemistry of Alkyl Nitrates, *J. Photochem. Photobiol. A*, 51, 281–292, 1990.
- Wang, J., Doussin, J. F., Perrier, S., Perraudin, E., Katrib, Y., Pangu, E., and Picquet-Varrault, B.: Design of a new multi-phase experimental simulation chamber for atmospheric photochemistry, aerosol and cloud chemistry research, *Atmos. Meas. Tech.*, 4, 2465–2494, <https://doi.org/10.5194/amt-4-2465-2011>, 2011.
- Xiong, F., Borca, C. H., Slipchenko, L. V., and Shepson, P. B.: Photochemical degradation of isoprene-derived 4,1-nitrooxy enal, *Atmos. Chem. Phys.*, 16, 5595–5610, <https://doi.org/10.5194/acp-16-5595-2016>, 2016.
- Zhu, T., Barnes, I., and Becker, K. H.: Relative-rate study of the gas-phase reaction of hydroxy radicals with difunctional organic nitrates at 298 K and atmospheric pressure, *J. Atmos. Chem.*, 13, 301–311, 1991.